

# Data-Driven Soft Decoding of Compressed Images in Dual Transform-Pixel Domain

Xianming Liu, *Member, IEEE*, Xiaolin Wu, *Fellow, IEEE*,  
Jiantao Zhou, *Member, IEEE*, and Debin Zhao, *Member, IEEE*

**Abstract**—In the large body of research literature on image restoration, very few papers were concerned with compression-induced degradations, although in practice, the most common cause of image degradation is compression. This paper presents a novel approach to restoring JPEG-compressed images. The main innovation is in the approach of exploiting residual redundancies of JPEG code streams and sparsity properties of latent images. The restoration is a sparse coding process carried out jointly in the DCT and pixel domains. The prowess of the proposed approach is directly restoring DCT coefficients of the latent image to prevent the spreading of quantization errors into the pixel domain, and at the same time, using online machine-learned local spatial features to regulate the solution of the underlying inverse problem. Experimental results are encouraging and show the promise of the new approach in significantly improving the quality of DCT-coded images.

**Index Terms**—Compressed image restoration, sparse coding, soft decoding, machine learning.

## I. INTRODUCTION

THE PAST decade has witnessed a rapid growth of research works on sparsity-based image analysis and processing. A large number of sparsity-based image restoration methods have been reported [2]–[11] that can deliver superior performance to previous techniques in various applications, e.g., image denoising, super-resolution (upsampling), deconvolution, demosaicking, etc. However, so far the sparsity-based image restoration approaches are seemingly not as effective

on combating compression artifacts as on other types of degradations.

Relatively fewer papers were devoted to sparsity-based restoration of compressed images [12]–[16], [28], [29]. This is quite regrettable, as the most common cause of image degradation in practice is nothing but compression. Sensor noises and low spatial resolution are much lesser problems nowadays because modern digital cameras, even mass-marketed ones, offer sufficiently high spatial/spectral resolutions and high signal-to-noise ratio (SNR) to meet the image quality requirements of most users. But compression is and will continue to be indispensable in almost all visual communication and computing systems, as the sheer volume of image data can easily overwhelm the communication bandwidth and in-device storage.

The so-far lack of success in sparsity-based restoration of compressed images is largely due to the fact that the compression noises are much more difficult to model than other degradation sources, e.g., motion blur and sensor noises. The non-linearity of quantization operations in image compression systems makes quantization noises *signal dependent*, far from being white and independent, as commonly assumed by works on other image restoration problems [17], [18], [20]. Following the tradition of assuming degradations to be signal independent, most existing works on restoration of compressed images modeled quantization noises as signal independent ones, e.g., uniform noises in DCT domain [21], white Gaussian noises (WGN) in spatial domain [22], [23], or generalized Gaussian noises [24]. Inaccurate modeling of compression degradations limits the restoration performance.

## A. Related Work

Up to now, very few published compressed image restoration techniques directly recover the original compressed DCT coefficients [24], [25]. Most of existing works on restoring compressed images are formulated to estimate the latent image in the pixel domain. Reeve and Lim proposed to remove structured discontinuities induced by DCT code blocks by Gaussian filtering of the pixels around the DCT block boundaries [26]. Zhai *et al.* employed postfiltering in shifted overlapped windows and fused the filtering results to better suppress blocking artifacts [27]. Restoration of JPEG-compressed images can be cast and solved in a standard inverse problem formulation. Alter *et al.* proposed a total variation (TV) minimization method constrained by the intervals of unquantized DCT coefficients [28], assuming that natural images are approximately

Manuscript received April 28, 2015; revised October 18, 2015, December 14, 2015, and January 8, 2016; accepted January 16, 2016. Date of publication February 8, 2016; date of current version February 26, 2016. This work was supported in part by the Major State Basic Research Development Program of China (973 Program) under Grant 2015CB351804, in part by the National Science Foundation of China under Grant 61300110, Grant 61331014 and Grant 61402547, in part by the Fundamental Research Funds for the Central Universities under Grant HIT. NSRIF. 2015067, in part by the Macau Science and Technology Development Fund under Grant FDCT/009/2013/A1 and Grant FDCT/046/2014/A1, and in part by the Research Committee at University of Macau under Grant MRG007/ZJT/2015/FST, Grant MRG021/ZJT/2013/FST, Grant MYRG2014-00031-FST and Grant MYRG2015-00056-FST. The associate editor coordinating the review of this manuscript and approving it for publication was Dr. Abd-Krim Karim Seghouane.

X. Liu and D. Zhao are with the School of Computer Science and Technology, Harbin Institute of Technology, Harbin 150001, China (e-mail: xmliu.hit@gmail.com; dbzhao@hit.edu.cn).

X. Wu is with the Department of Electrical and Computer Engineering, McMaster University, ON, Canada, L8S 4K1; and also with the Department of Electrical Engineering, Shanghai Jiao Tong University, Shanghai 200240, China (e-mail: xwu@ece.mcmaster.ca).

J. Zhou is with the Department of Computer and Information Science, Faculty of Science and Technology, University of Macau, Macau 999078, China (e-mail: jtzhou@umac.mo).

Color versions of one or more of the figures in this paper are available online at <http://ieeexplore.ieee.org>.

Digital Object Identifier 10.1109/TIP.2016.2526910

piecewise constant. Their design goal is to reduce blocking artifacts and Gibbs phenomenon while preserving sharp edges. Bredies and Holler studied optimality conditions of the TV minimization approach in an infinite dimensional model, and proposed to solve a discrete version by a primal-dual algorithm supplemented by a primal-dual gap stopping criterion [29]. Accompanying its success in other restoration applications, the approach of sparse coding has also shown its promise in combating compression distortions [12]–[16]. Very recently, Kwon *et al.* [30] proposed a simplified scheme of Gaussian process regression that can be applied to the removal of compression artifacts among other applications.

### B. Our Contribution

In this work, we do away with any preassumption on compression noises and aim to repair signal-dependent degradations via a novel data-driven approach. The proposed restoration approach performs a joint sparse coding in both the DCT domain and the pixel domain. As natural images are statistically non-stationary with spatially varying sparse representations, sparse coding is performed on individual patches, one at a time, so that the restoration can adapt to local statistics. For each restoration patch, two dictionaries of PCA bases are learned in the DCT and the pixel domains respectively, using sample sets of approximately matched DCT code blocks. The two dictionaries are then used to generate two locally adaptive sparse representations that jointly determine the restored image patch. Fig. 1 depicts the architecture of the proposed image restoration framework, in which the degraded input is the decompressed (hard-decoded) image and the restored output is called soft-decoded image. In the compression literature, the task of repairing hard-decoded results is commonly referred to as soft decoding.

The premise of soft decoding is that practical image compression methods, such as popular international standards JPEG, H.264/AVC, HEVC etc., are not information-theoretically optimal. Therefore, the resulting compression code streams still contain residual redundancies. It is possible, at least theoretically, to improve the reconstruction by reestimating the original signal with the knowledge ignored or underused by the encoder. In particular, in the ubiquitous local DCT block-based coding framework, correlations exist between different code blocks, because natural images tend to have similar local structures and the code block size is not large enough to capture the underlying statistical redundancy. These inter-block correlations, which are not exploited by the encoder, can be used by the decoder to increase the reconstruction fidelity without receiving any extra bits.

The restoration of compressed images either in the pixel or in the DCT domain alone has its own drawbacks. As the pixel domain restoration works with hard-decoded image, the inverse DCT is required. This will propagate an isolated quantization error, originally confined to a single DCT coefficient, to all pixels in the corresponding DCT block. To make the matter worse, an aggressively quantized DCT coefficient can produce structured errors in the pixel domain that correlate to the latent signal, complicating the restoration task. On the other hand, the pure DCT-domain restoration is

severely restricted by the fact that the compression process sets most of the high frequency coefficients to zero, making the recovery of edges and fine textures impossible. In the proposed dual domain soft decoding (D2SD) scheme, the advantages and disadvantages of the pixel-domain and DCT-domain restorations are made to complement each other. The design motive, which is also a main contribution of this work, is to exploit residual redundancies (e.g., inter-DCT-block correlations) in the DCT domain without spreading errors into the pixel domain, and at the same time recover high frequency information with machine learning driven by a large training set. A uniqueness of our machine learning method for soft decoding is in its feature selection: the DCT code block rather than the (or some attributes of) corresponding hard-decoded pixel patch is used as the feature vector. Directly associating the DCT code block to the underlying latent image block isolates the degradation cause at its root and hence simplifies the learning task. Furthermore, the soft decoding performance is boosted by incorporating the known boundaries of quantizer cells, which is a strong piece of available side information in the DCT code stream, into the new sparsity-based restoration scheme. The short version of this work was presented in [1].

The rest of the paper is organized as follows. Section II details the proposed technique of sparse coding in the DCT domain; here the main novelty is the collecting and clustering of a sample set created by performing forward DCT of overlapped pixel patches in the hard-decoded image. By breaking free from the rigid DCT code block tessellation, the proposed sparse coding process can fully benefit from the self-similarities of the latent image and remove the blocking compression artifacts. In Section III, we extend sparse coding from the DCT domain to the dual DCT-pixel domain, and finally cast the dual sparse coding-based restoration of compressed images as a mixed  $\ell_1$ - $\ell_2$  minimization problem. The highlight of this section is the new data-driven learning method for repairing distorted high-frequency image features. Section IV provides the details of solving the formulated optimization problem, and Section V reports the experimental results. We finally conclude in Section VI.

## II. SPARSITY-BASED SOFT DECODING IN THE TRANSFORM DOMAIN

As mentioned earlier in the Introduction, soft decoding performed solely in the pixel domain has one main drawback: the inverse DCT has to be applied, which causes propagation of an isolated quantization error to all the pixels of the corresponding DCT block. In contrast, the soft decoding directly performed over the DCT coefficients can effectively avoid such problem, confining the quantization errors to the associated DCT coefficients.

In this section, we discuss the sparsity-based soft decoding in the transform domain, where adaptive dictionary learning in the DCT domain and a collaborative sparse coding mechanism to exploit inter-block correlations are involved. This DCT-domain restoration framework will be combined appropriately with the pixel-domain soft decoding in the next Section to eventually give our dual transform-pixel domain soft decoding approach.

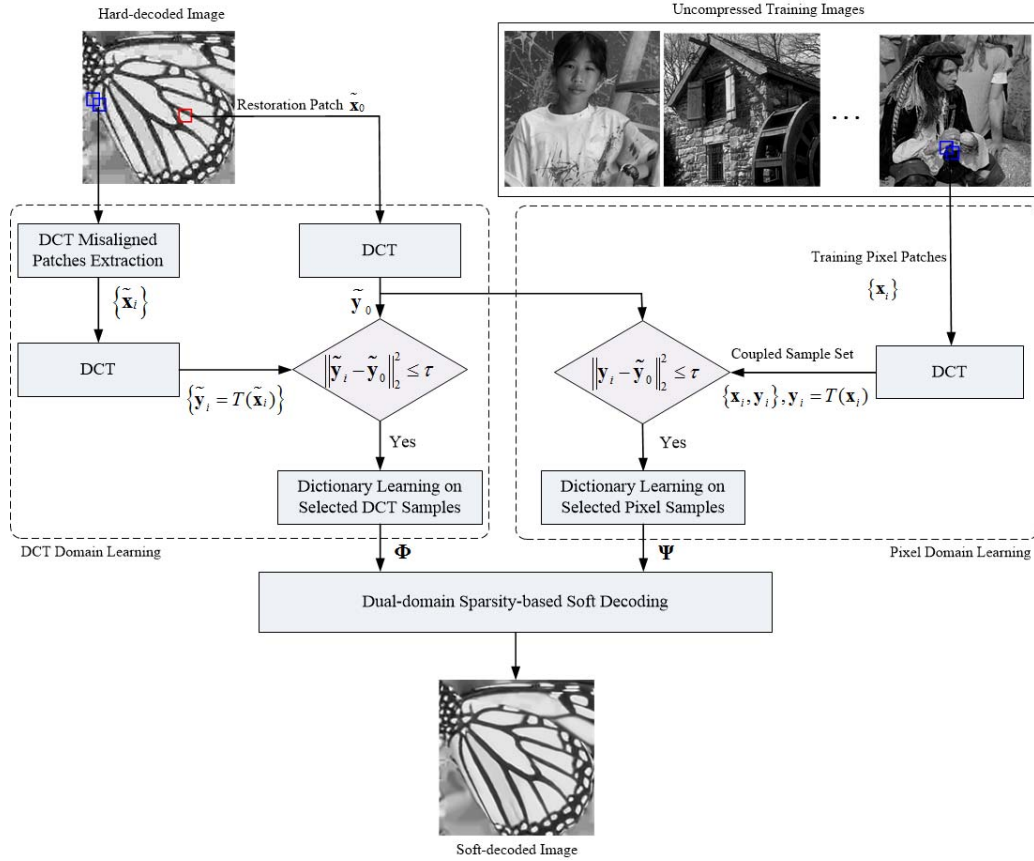


Fig. 1. Block diagram of the proposed data-driven soft decoding system in dual transform-pixel domain. In the hard-decoded image, the red block represents a coding block. The blue blocks represent non-coding blocks, which are exacted in an overlapped fashion. Note that for coding blocks, their DCT codes are read directly from the code stream. While for non-coding blocks, we perform DCT transform to get the corresponding DCT codes. Here, for simplicity we use “DCT” to cover both cases.

### A. Adaptive DCT Dictionary Learning

In JPEG compression images are coded in non-overlapping  $8 \times 8$  blocks in DCT domain; these blocks are called coding blocks in the sequel. As illustrated in Fig. 1, we divide the hard-decoded image  $\mathbf{H}$  into a set of *overlapped* patches  $\{\tilde{\mathbf{x}}_i\}$  of size  $8 \times 8$ , which is called non-coding blocks. For coding blocks, the DCT coefficients are read directly from the code stream. While for non-coding blocks, we apply the DCT transform on them to get the associated DCT coefficients, which are denoted as  $\{\tilde{\mathbf{y}}_i\}$ . We emphasize that blocks  $\{\tilde{\mathbf{x}}_i\}$  are extracted in overlapped positions in misalignment with the DCT coding block boundaries. The purpose is to destroy artificial block structures of JPEG compression method and hence remove much of the notorious DCT blocking artifacts.

To build the sparsity dictionary for restoring a generic DCT coefficient patch  $\tilde{\mathbf{y}}_0$ , we specifically employ the non-local self-similarity inherent to natural images and form the training set by

$$\mathcal{Y} = \{\tilde{\mathbf{y}}_i \mid \|\tilde{\mathbf{y}}_i - \tilde{\mathbf{y}}_0\|_2 \leq \tau\}, \quad (1)$$

where  $\tau$  is selected in practice such that the first  $n$  (we empirically set  $n = 30$ ) closest  $\tilde{\mathbf{y}}_i$  to  $\tilde{\mathbf{y}}_0$  constitute the training set  $\mathcal{Y}$ .

We make the vectors of collected patches to be the columns of matrix  $\mathbf{Y} \in \mathbb{R}^{64 \times n}$ . Then, following the work [4], we learn an adaptive sub-dictionary  $\Phi$  that is most relevant to  $\mathbf{Y}$  by applying PCA on  $\mathbf{Y}$ . PCA generates the dictionary  $\Phi$  whose atoms are the eigenvectors of the covariance matrix of  $\mathbf{Y}$ . In this way, we construct one sub-dictionary per DCT patch in an adaptive manner.

### B. Soft Decoding in the Transform Domain

All the existing image/video compression methods utilizing block-based DCT suffer from a common problem: DCT blocks are encoded independently, which could leave inter-block correlations. Such dependence not only reduces the coding efficiency, but also limits the modeling capability of sparsity-based image prior. This problem is aggravated for low bit rates as vital structural information of the source image is lost or severely distorted due to the quantization operations. An effective way of alleviating the above problem is to impose structural sparsity constraints when conducting soft decoding. Noticing that similar patches are often encoded by similar sparsity patterns, we in this work propose a *collaborative sparse coding* scheme, which explicitly introduces a regularization term to preserve the consistency of sparse codes for similar local patches. More specifically, the soft decoding in

the transform domain can be cast into the following minimization problem:

$$\begin{aligned} \min_{\{\alpha_i\}} \sum_i \|\tilde{\mathbf{y}}_i - \Phi_i \alpha_i\|_2^2 + \lambda_1 \sum_i \|\alpha_i\|_1 \\ + \frac{\gamma_1}{2} \sum_{i,j} \|\alpha_i - \alpha_j\|_2^2 \mathbf{W}_{ij}, \end{aligned} \quad (2)$$

where  $\lambda_1$  and  $\gamma_1$  are regularization parameters;  $\mathbf{W}_{ij}$  measures the similarity between a pair of patches  $(\tilde{\mathbf{y}}_i, \tilde{\mathbf{y}}_j)$  and can be defined by

$$\mathbf{W}_{ij} = \exp \left\{ -\frac{\|\tilde{\mathbf{y}}_i - \tilde{\mathbf{y}}_j\|_2^2}{\sigma^2} \right\}. \quad (3)$$

In addition to sparsity prior, the DCT image code stream contains another source of side information that should be exploited to further improve restoration performance. For each DCT coefficient  $\tilde{\mathbf{y}}_i(u, v)$ , where  $u$  and  $v$  are the indices of the corresponding 2D subband in DCT domain, we know exactly the associated quantization interval  $(q_{u,v}^L, q_{u,v}^U)$  in which  $\tilde{\mathbf{y}}_i(u, v)$  lies in. Namely,

$$q_{u,v}^L \leq \tilde{\mathbf{y}}_i(u, v) \leq q_{u,v}^U, \quad (4)$$

holds for all  $u$  and  $v$ . Note that such important side information is available without the need of receiving any extra bits. These linear inequalities can be incorporated into (2) to confine the solution space, which could further improve the restoration performance. For non-coding blocks, the quantization interval of the corresponding similar coding block is used as the constraint. Finally, we formulate our problem of soft decoding in the transform domain as the following constrained optimization problem:

$$\begin{aligned} \min_{\{\alpha_i\}} \sum_i \|\tilde{\mathbf{y}}_i - \Phi_i \alpha_i\|_2^2 + \lambda_1 \sum_i \|\alpha_i\|_1 \\ + \frac{\gamma_1}{2} \sum_{i,j} \|\alpha_i - \alpha_j\|_2^2 \mathbf{W}_{ij}, \\ \text{s.t. } \mathbf{q}^L \leq \Phi_i \alpha_i \leq \mathbf{q}^U, \end{aligned} \quad (5)$$

where  $\mathbf{q}^L$  and  $\mathbf{q}^U$  are vectors containing bound values of the quantization interval, and  $\leq$  denotes the element-wise inequality.

### III. SPARSITY-BASED SOFT DECODING IN DUAL TRANSFORM-PIXEL DOMAIN

In this section, we propose to augment the previously discussed transform-domain restoration by including the pixel-domain knowledge. The standalone restoration in the DCT domain cannot satisfactorily recover the high-frequency components that are discarded or severely distorted during the quantization process. In this work, we address this challenging issue by using a machine learning-based technique that incorporates high-frequency priors of uncompressed images into the restoration framework. Specifically, we develop a novel soft decoding strategy in dual transform-pixel domain in such a way that the advantages and disadvantages of both domains can complement each other. In the following, we first present the adaptive dictionary learning in the pixel domain,

and then describe the dual transform-pixel domain strategy of soft decoding.

#### A. Adaptive Dictionary Learning in the Pixel Domain

The learning in the pixel domain employs a training set of uncompressed images, from which we extract pairs of patches in both the pixel and the DCT domains. Specifically, let  $\{\mathbf{x}_i\}$  be the  $8 \times 8$  sized pixel blocks from the uncompressed training images, and let  $\{\mathbf{y}_i\}$  be the corresponding DCT coefficient blocks. To restore a generic pixel patch  $\tilde{\mathbf{x}}_0$ , whose DCT counterpart is denoted by  $\tilde{\mathbf{y}}_0$ , we construct a dictionary by using the training data in the paired set  $\{\mathbf{x}_i, \mathbf{y}_i\}$ . We collect a set of pixel patches  $\mathbf{x}_i$  that have their DCT representations sufficiently close to  $\tilde{\mathbf{y}}_0$ :

$$\mathcal{X} = \{\mathbf{x}_i \mid \|\mathbf{y}_i - \tilde{\mathbf{y}}_0\|_2^2 \leq \tau\}, \quad (6)$$

Similar to the dictionary learning in the DCT domain, we can apply the PCA-based technique over  $\mathcal{X}$  to obtain the dictionary  $\Psi_i$ .

When selecting the samples in (6), it should be noted that we directly employ the DCT code block rather than the corresponding hard-decoded pixel patch as the feature vector. Directly associating the DCT code block to the underlying latent image block isolates the degradation cause at its root and hence can significantly simplify the learning task and improve the restoration performance. In addition, we here use the original, unquantized  $\{\mathbf{y}_i\}$  to calculate the  $\ell_2$  distances for training sample selection. A better alternative to this end is to use the quantized version of  $\{\mathbf{y}_i\}$ , and obtain the set  $\mathcal{X}$  for each quantization parameter. We experimentally find that this strategy indeed improves the overall performance; but the additional gain over the case of using the unquantized  $\{\mathbf{y}_i\}$  is rather limited (less than 0.1dB). Meanwhile, the incurred complexity is large and the flexibility of performing the soft decoding is reduced. Therefore, in this work we still adopt the simple yet effective way of selecting the samples, as demonstrated in (6).

#### B. Soft Decoding in Dual Domain

Given the two learned dictionaries  $\Phi = \{\Phi_i\}$  and  $\Psi = \{\Psi_i\}$  in the transform and the pixel domain, we jointly search for two sparse code vectors  $\{\alpha_i\}$  and  $\{\beta_i\}$  that best represent the observed DCT patches  $\{\tilde{\mathbf{y}}_i\}$  in the dual domain:

$$\begin{aligned} \arg \min_{\{\alpha_i, \beta_i\}} \left\{ \sum_i \|\tilde{\mathbf{y}}_i - \Phi_i \alpha_i\|_2^2 + \lambda_1 \sum_i \|\alpha_i\|_1 \right. \\ \left. + \lambda_3 \sum_i \|\mathbf{T}^{-1} \Phi_i \alpha_i - \Psi_i \beta_i\|_2^2 + \lambda_2 \sum_i \|\beta_i\|_1 \right\} \\ \text{s.t. } \mathbf{q}^L \leq \Phi_i \alpha_i \leq \mathbf{q}^U, \end{aligned} \quad (7)$$

where  $\mathbf{T}^{-1}$  is the inverse DCT;  $\lambda_1, \lambda_2, \lambda_3$  are Lagrange multipliers.

Incorporating the collaborative sparse coding and the quantization interval constraint into (7), we arrive at the following

constrained optimization problem to estimate  $\{\alpha_i\}$  and  $\{\beta_i\}$ :

$$\arg \min_{\{\alpha_i, \beta_i\}} \left\{ \begin{array}{l} \sum_i \|\tilde{\mathbf{y}}_i - \Phi_i \alpha_i\|_2^2 + \lambda_1 \sum_i \|\alpha_i\|_1 \\ + \frac{\gamma_1}{2} \sum_{i,j} \|\alpha_i - \alpha_j\|_2^2 \mathbf{W}_{ij} \\ + \lambda_3 \sum_i \|\mathbf{T}^{-1} \Phi_i \alpha_i - \Psi_i \beta_i\|_2^2 \\ + \lambda_2 \sum_i \|\beta_i\|_1 + \frac{\gamma_2}{2} \sum_{i,j} \|\beta_i - \beta_j\|_2^2 \mathbf{W}_{ij} \end{array} \right\},$$

s.t.  $\mathbf{q}^L \preceq \Phi_i \alpha_i \preceq \mathbf{q}^U$ , (8)

where  $\gamma_1, \gamma_2$  are two other Lagrange multipliers. Note that here we apply the collaborative sparse coding in both the DCT and the pixel domains. Joint restoration in the DCT and the pixel domain allows the two sparse representations  $\{\alpha_i\}$  in dictionary  $\Phi$  and  $\{\beta_i\}$  in dictionary  $\Psi$  to cross validate each other, improving the quality of soft decoded image patches.

Upon solving (11) and obtaining the optimal sparse coding vectors  $\{\beta_i^*\}$  in the pixel domain, the soft-decoded image  $\hat{\mathbf{H}}$  can be obtained by averaging all the reconstructed patches [2]:

$$\hat{\mathbf{H}} = \left( \sum_{i=1}^N \mathbf{R}_i^T \mathbf{R}_i \right)^{-1} \left( \sum_{i=1}^N \mathbf{R}_i^T \Psi_i \beta_i^* \right), \quad (9)$$

where  $N$  is the total number of sampled patches,  $\mathbf{R}_i$  is the matrix extracting patch  $\tilde{\mathbf{x}}_i$  from the hard-decoded image  $\mathbf{H}$  at location  $i$ .

#### IV. OPTIMIZATION DETAILS

In this section, we present the details of solving the constrained optimization problem in (8).

The objective function Eq.(8) can be further reformulated into a matrix form:

$$\arg \min_{\{\mathbf{A}, \mathbf{B}\}} \left\{ \begin{array}{l} \|\tilde{\mathbf{Y}} - \Phi \mathbf{A}\|_2^2 + \lambda_1 \|\mathbf{A}\|_1 + \gamma_1 \text{Tr}(\mathbf{A} \mathbf{L} \mathbf{A}^T) \\ + \lambda_3 \|\mathbf{T}^{-1} \Phi \mathbf{A} - \Psi \mathbf{B}\|_2^2 + \lambda_2 \|\mathbf{B}\|_1 \\ + \gamma_2 \text{Tr}(\mathbf{B} \mathbf{L} \mathbf{B}^T) \end{array} \right\},$$

s.t.  $\mathbf{Q}^L \preceq \Phi \mathbf{A} \preceq \mathbf{Q}^U$ , (10)

where  $\tilde{\mathbf{Y}} \in \mathbb{R}^{64 \times N}$  is the DCT patch sample matrix,  $N$  is the number of blocks to be processed,  $\text{Tr}(\cdot)$  denotes the trace function,  $\mathbf{L}$  is the graph-Laplacian matrix [32], [33],  $\mathbf{A}$  and  $\mathbf{B}$  are sparse codes matrices,  $\mathbf{Q}^L$  and  $\mathbf{Q}^U$  are matrices with  $\mathbf{q}^L$  and  $\mathbf{q}^U$  being columns, respectively.

Defining  $\Theta = [\mathbf{A} \ \mathbf{B}]^T = \{\alpha_i, \beta_i\}^T$ ,  $\theta_i = (\alpha_i, \beta_i)^T$ ,  $\hat{\mathbf{Y}} = [\tilde{\mathbf{Y}} \ \mathbf{0}]^T = \{\hat{\mathbf{y}}_i\}$ ,  $\mathbf{D} = \begin{bmatrix} \Phi & \mathbf{0} \\ -\sqrt{\lambda_3} \mathbf{T}^{-1} \Phi & \sqrt{\lambda_3} \Psi \end{bmatrix}$ , and  $\hat{\mathbf{L}} = \begin{bmatrix} \gamma_1 \mathbf{L} & \mathbf{0} \\ \mathbf{0} & \gamma_2 \mathbf{L} \end{bmatrix}$ , the optimization problem in (10) can be simplified as

$$\arg \min_{\Theta} \|\hat{\mathbf{Y}} - \mathbf{D} \Theta\|_F^2 + \lambda \|\Theta\|_1 + \gamma \text{Tr}(\Theta^T \hat{\mathbf{L}} \Theta),$$

s.t.  $[\mathbf{Q}^L \ \mathbf{0}]^T \preceq \mathbf{D} \Theta \preceq [\mathbf{Q}^U \ \mathbf{0}]^T$ , (11)

where for simplicity we set  $\lambda = \lambda_1 = \lambda_2$  and  $\gamma = \gamma_1 = \gamma_2$ . This is a mixed  $\ell_1$ - $\ell_2$  minimization problem with a graph-Laplacian regularization term.

It is easy to see that the objective function in (11) is convex, which implies that global minimizer exists and is unique.

#### Algorithm 1 Optimization Algorithm for Estimating Sparse Coefficients

**Input:** The observed DCT patches  $\hat{\mathbf{y}}_i$ ; the dictionary  $\mathbf{D}_i$ ; the graph-Laplacian matrix  $\hat{\mathbf{L}}_i$ ;  $\lambda, \gamma$ ;

**Output:** The optimal sparse code  $\theta_i^*$ .

**Procedure:**

**Initialize Step:**

- 1:  $\theta_i$  is the result of standard sparse coding [38], active set  $\mathcal{A} := \text{Find}(\theta_i \neq 0)$ ,  $\mathbf{s} := \text{sign}(\theta_i)$ ,  $\mathbf{s}_j \in \{-1, 0, 1\}$  denotes  $\text{sign}(\theta_i^{(j)})$ , where  $\theta_i^{(j)}$  is  $j$ -th component of  $\theta_i$ ;

**Activate Step:**

- 2: From zero coefficient of  $\theta_i$ , select  $j = \arg \max_j \left| \nabla_i^{(j)} J(\theta_i) \right|$ , where  $\nabla_i^{(j)} J(\theta_i)$  the subdifferentiable value of the  $j$ th coefficient of  $J(\theta_i)$ . Activate  $\theta_i^{(j)}$  only if it locally improve the objective function Eq.(13), namely:
  - If  $\nabla_i^{(j)} J(\theta_i) > \lambda$ , then set  $\mathbf{s}_j = -1$ ,  $\mathcal{A} = \{j\} \cup \mathcal{A}$
  - If  $\nabla_i^{(j)} J(\theta_i) < -\lambda$ , then set  $\mathbf{s}_j = 1$ ,  $\mathcal{A} = \{j\} \cup \mathcal{A}$ .

**Feature-sign Step:**

- 3: Let  $\hat{\mathbf{D}}_i$  be a submatrix of  $\mathbf{D}_i$  that only contains columns corresponding to the active set. Let  $\theta_i$ ,  $\hat{\mathbf{h}}_i$  and  $\hat{\mathbf{s}}$  be subvectors of  $\theta_i$ ,  $\mathbf{h}_i$  and  $\mathbf{s}$  corresponding to the active set;
- 4: Compute the optimal solution under the current active set:

$$\widehat{\theta}_i^{new} = \left( \hat{\mathbf{D}}_i^T \hat{\mathbf{D}}_i + \gamma \hat{\mathbf{L}}_{ii} \mathbf{I} \right)^{-1} \left( \hat{\mathbf{D}}_i^T \hat{\mathbf{y}}_i - (\lambda \hat{\theta}_i + \hat{\mathbf{h}}_i) / 2 \right) \quad (14)$$

where  $\mathbf{I}$  is the identity matrix;

- 5: Perform a discrete line search on the closed line segment from  $\hat{\theta}_i$  to  $\hat{\theta}_i^{new}$ : Check the objective value at  $\hat{\theta}_i^{new}$  and all points where any coefficient changes sign, and update  $\hat{\theta}_i$  to the point with lowest objective value;
- 6: Remove zero coefficients of  $\hat{\theta}_i$  from the active set and update  $\mathbf{s} = \text{sign}(\hat{\theta}_i)$ ;
- Check the Optimality Conditions Step:**
- 7: Condition (a): Check optimality condition for nonzero coefficients:  $\left| \nabla_i^{(j)} J(\theta_i) \right| + \lambda \text{sign}(\theta_i^{(j)}) = 0, \forall \theta_i^{(j)} \neq 0$ . If condition (a) is satisfied, go to feature-sign step; else check condition (b).
- 8: Condition (b): Check optimality condition for zero coefficients:  $\left| \nabla_i^{(j)} J(\theta_i) \right| \leq \lambda, \forall \theta_i^{(j)} = 0$ . If condition (b) is satisfied, go to activate step; else return  $\theta_i$  as the solution denoted as  $\theta_i^*$ ;

Several approaches have been proposed to solve the problem of this form [34], [35]. In this paper, we use an optimization method based upon coordinate descent to solve this problem. We optimize each code  $\theta_i$  individually while keeping all the remaining sparse representation codes  $\theta_j (j \neq i)$  fixed. We further define:

$$\begin{aligned} J(\Theta) &= \|\hat{\mathbf{Y}} - \mathbf{D} \Theta\|_F^2 + \gamma \text{Tr}(\Theta^T \hat{\mathbf{L}} \Theta) \\ &= \sum_i \|\hat{\mathbf{y}}_i - \mathbf{D}_i \theta_i\|_2^2 + \gamma \sum_{i,j} \hat{\mathbf{L}}_{ij} \theta_i^T \theta_j. \end{aligned} \quad (12)$$

We can obtain  $\theta_i$  by solving the following optimization problem:

$$\begin{aligned} \arg \min_{\theta_i} J(\theta_i) + \lambda \|\theta_i\|_1 \\ = \arg \min_{\theta_i} \|\hat{\mathbf{y}}_i - \mathbf{D}_i \theta_i\|_2^2 + \gamma \hat{\mathbf{L}}_{ii} \theta_i^T \theta_i + \theta_i^T \mathbf{h}_i + \lambda \sum_k \left| \theta_i^{(k)} \right|, \end{aligned} \quad (13)$$

where  $\mathbf{h}_i = 2\gamma (\sum_{j \neq i} \hat{\mathbf{L}}_{ij} \theta_j)$ ,  $\theta_i^{(k)}$  is the  $k$ -th element of  $\theta_i$ .

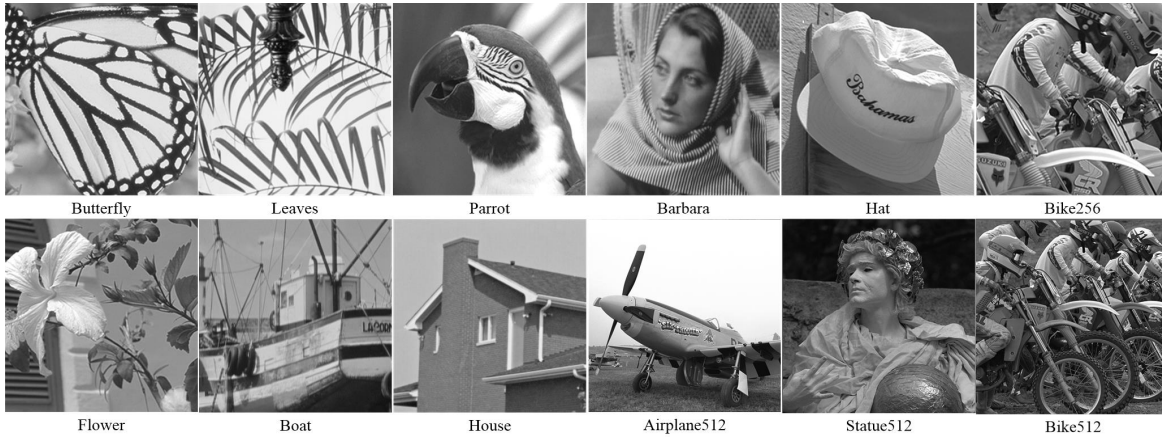


Fig. 2. Twelve test images, the first nine images are  $256 \times 256$ , the last three ones are  $512 \times 512$ .

TABLE I  
OBJECTIVE QUALITY COMPARISON WITH RESPECT TO PSNR (IN dB) AND SSIM AT QF = 5

Images	JPEG		ACR		PSW		BM3D-SAPCA		KSVD		DicTV		D2SD	
	PSNR	SSIM	PSNR	SSIM	PSNR	SSIM	PSNR	SSIM	PSNR	SSIM	PSNR	SSIM	PSNR	SSIM
<i>Butterfly</i>	22.65	0.7571	22.55	0.7636	23.58	0.8152	23.91	0.8266	23.96	0.8417	23.54	0.8228	<b>25.15</b>	<b>0.8705</b>
<i>Barbara</i>	23.85	0.6562	24.01	0.6698	24.73	0.6958	24.76	0.7051	24.93	0.7091	24.49	0.7006	<b>25.48</b>	<b>0.7261</b>
<i>Boat</i>	25.23	0.7054	25.19	0.7053	26.13	0.7382	26.31	0.7547	26.64	0.7656	26.31	0.7491	<b>26.98</b>	<b>0.7758</b>
<i>Leaves</i>	22.49	0.7775	22.42	0.7765	23.49	0.8276	23.78	0.8408	23.76	0.8481	23.27	0.8245	<b>24.92</b>	<b>0.8831</b>
<i>Bike</i>	21.72	0.6530	21.61	0.6448	22.16	0.6743	22.60	0.7039	22.56	0.6976	22.28	0.6952	<b>23.08</b>	<b>0.7203</b>
<i>Flower</i>	24.51	0.6866	24.43	0.7636	25.19	0.7078	25.49	0.7352	25.39	0.7366	25.88	0.7316	<b>25.88</b>	<b>0.7501</b>
<i>House</i>	27.76	0.7732	27.77	0.7756	28.73	0.7964	28.87	0.8020	28.47	0.8168	29.59	0.8072	<b>29.95</b>	<b>0.8217</b>
<i>Hat</i>	25.97	0.7117	26.11	0.7328	26.84	0.7557	26.79	0.7497	27.06	0.7721	27.33	0.7707	<b>27.28</b>	<b>0.7741</b>
<i>Parrot</i>	26.15	0.7851	26.49	0.8032	27.08	0.8275	27.40	0.8329	27.22	0.8465	27.92	0.8382	<b>28.04</b>	<b>0.8504</b>
<i>Airplane512</i>	26.01	0.7753	26.45	0.7929	27.01	0.8086	27.11	0.8101	27.38	0.8204	26.95	0.8114	<b>28.92</b>	<b>0.8407</b>
<i>Bike512</i>	22.11	0.6198	22.20	0.6184	22.80	0.6422	23.12	0.6693	23.13	0.6597	22.74	0.6562	<b>24.76</b>	<b>0.6949</b>
<i>Statue512</i>	25.64	0.6735	25.99	0.6908	26.54	0.7143	26.58	0.7077	26.85	0.7293	26.51	0.7269	<b>28.11</b>	<b>0.7630</b>
Average	24.51	0.7145	24.60	0.7281	25.35	0.7503	25.56	0.7615	25.61	0.7702	25.56	0.7612	<b>26.55</b>	<b>0.7892</b>

The solution of (13) can be effectively obtained by the feature-sign search algorithm [36]. The optimization algorithm is detailed in **Algorithm 1**; more information about the optimization process can be found in [34] and [35]. To satisfy the quantization bin constraints, we simply clip DCT coefficients outside the bin to the nearest bin boundaries.

## V. EXPERIMENTAL RESULTS

In this section, experimental results are presented to demonstrate the superior performance of the proposed dual-domain joint estimation approach for restoring compressed images.

### A. Comparison Group

The proposed approach is compared with the state-of-the-art methods in the literature. The comparison group is

composed of: 1) deblocking methods: the ACR algorithm [37], the PSW algorithm [27]. These methods are included into the comparison group because they can be considered as soft decoding methods for DCT-compressed images; 2) denoising algorithms: the extended work BM3D-SAPCA [19] of the well-known BM3D algorithm [18], which achieves better performance than BM3D. BM3D-SAPCA is included because the restoration of compressed images can be viewed as a denoising process, in which the degradation source is the quantization; 3) sparsity-based restoration methods: the well-known KSVD [17], DicTV [14], and the proposed dual-domain soft decoding (D2SD) algorithm. DicTV is a very latest sparsity-based compressed image restoration algorithm. All the source codes of the compared algorithms are kindly provided by their authors. The source code of our method is available at <http://homepage.hit.edu.cn/pages/xmliu/2>.

TABLE II  
OBJECTIVE QUALITY COMPARISON WITH RESPECT TO PSNR (IN dB) AND SSIM AT QF = 80

Images	JPEG		ACR		PSW		BM3D-SAPCA		KSVD		DicTV		D2SD	
	PSNR	SSIM	PSNR	SSIM	PSNR	SSIM	PSNR	SSIM	PSNR	SSIM	PSNR	SSIM	PSNR	SSIM
<i>Butterfly</i>	34.75	0.9639	34.60	0.9613	34.75	0.9639	36.17	0.9761	35.53	0.9711	34.70	0.9684	<b>37.13</b>	<b>0.9806</b>
<i>Barbara</i>	37.61	0.9737	37.58	0.9734	37.59	0.9737	38.66	0.9774	38.32	0.9742	36.01	0.9570	<b>39.34</b>	<b>0.9795</b>
<i>Boat</i>	38.37	0.9658	38.29	0.9649	38.37	0.9662	39.60	0.9728	39.02	0.9672	35.56	0.9486	<b>39.46</b>	<b>0.9728</b>
<i>Leaves</i>	35.91	0.9789	35.81	0.9774	35.90	0.9788	38.02	0.9914	37.30	0.9871	35.85	0.9835	<b>39.04</b>	<b>0.9920</b>
<i>Bike</i>	34.44	0.9676	34.48	0.9676	34.48	0.9676	35.59	0.9773	35.27	0.9737	33.91	0.9559	<b>36.45</b>	<b>0.9802</b>
<i>Flower</i>	36.14	0.9616	36.13	0.9607	36.17	0.9618	37.36	0.9718	36.86	0.9663	34.82	0.9444	<b>37.86</b>	<b>0.9733</b>
<i>House</i>	39.10	0.9530	39.05	0.9621	39.10	0.9532	40.04	0.9549	39.26	0.9447	37.29	0.9231	<b>40.78</b>	<b>0.9643</b>
<i>Hat</i>	37.08	0.9567	37.14	0.9563	37.19	0.9582	38.13	0.9628	37.58	0.9537	35.93	0.9350	<b>38.65</b>	<b>0.9672</b>
<i>Parrot</i>	38.18	0.9621	38.27	0.9621	38.28	0.9627	38.81	0.9626	38.43	0.9587	36.67	0.9443	<b>39.30</b>	<b>0.9663</b>
<i>Airplane512</i>	37.98	0.9648	37.92	0.9643	38.00	0.9653	38.96	0.9694	38.56	0.9663	36.69	0.9429	<b>40.09</b>	<b>0.9727</b>
<i>Bike512</i>	34.78	0.9654	34.78	0.9654	34.78	0.9655	35.93	0.9751	35.57	0.9707	33.88	0.9476	<b>37.56</b>	<b>0.9775</b>
<i>Statue512</i>	37.21	0.9550	37.21	0.9550	37.22	0.9555	37.94	0.9575	37.35	0.9489	35.32	0.9191	<b>39.24</b>	<b>0.9650</b>
Average	36.79	0.9640	36.771	0.9642	36.81	0.9643	37.93	0.9707	37.42	0.9652	35.55	0.9474	<b>38.74</b>	<b>0.9742</b>

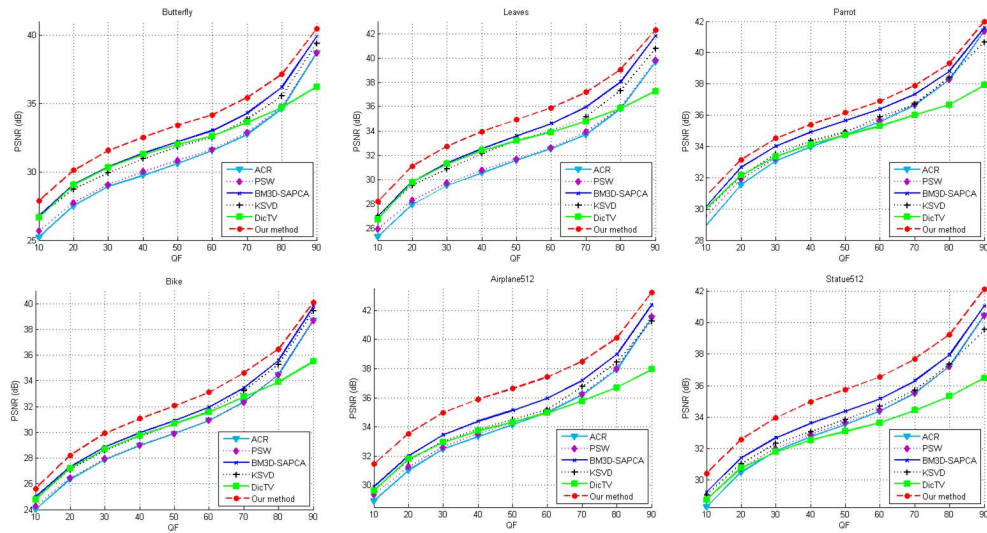


Fig. 3. QF-PSNR performance comparison for QFs ranging from 10 to 90.

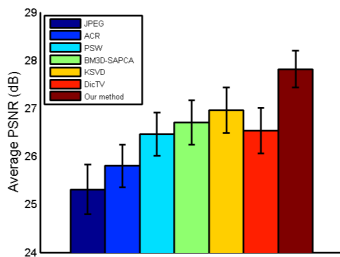


Fig. 4. Average PSNR values comparison of tested methods in a large image test set at QF = 5. The  $p$ -value in F-TEST is 5.7129e-12.

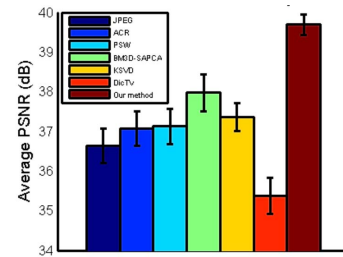


Fig. 5. Average PSNR values comparison of tested methods in a large image test set at QF = 80. The  $p$ -value in F-TEST is 8.0875e-35.

For thoroughness of our comparison study, we select twelve widely used images in the literature as test images, as illustrated in Fig. 2. The first nine images are of size  $256 \times 256$ ,

the last three ones are of size  $512 \times 512$ . For the uncompressed training set used to get the pixel-domain dictionary, we randomly select five images from the Kodak Lossless True Color

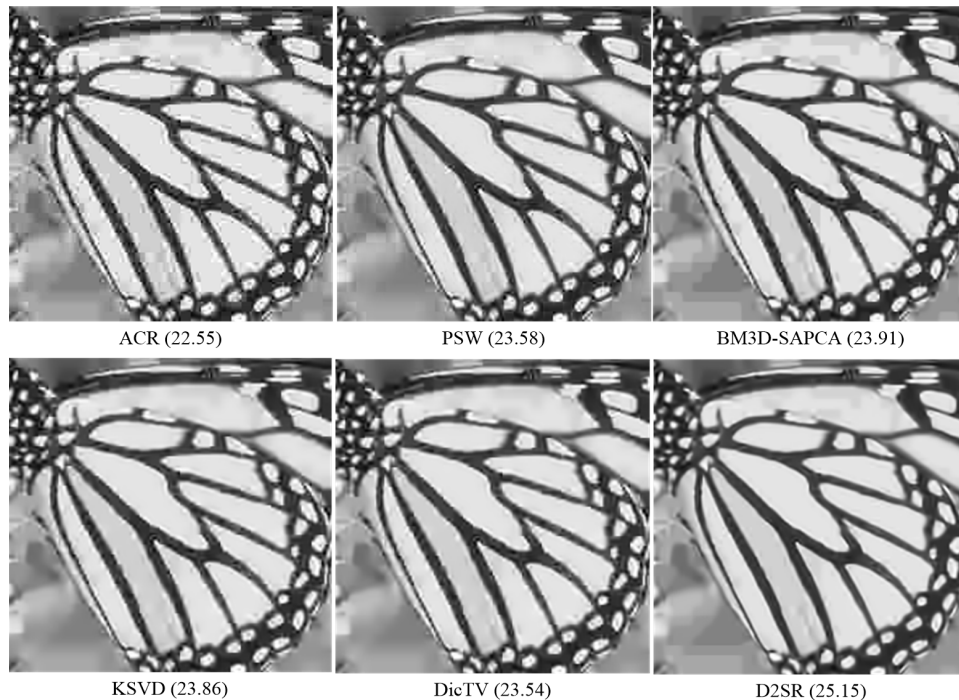


Fig. 6. Comparison of tested methods in visual quality on *Butterfly* at  $QF = 5$ . The corresponding PSNR values (in dB) are also shown.

Image Suite.<sup>1</sup> Certainly, the training set does not have any overlap with the test set.

### B. Objective Performance Comparison

Table I-II tabulate the PSNR and SSIM results of the above algorithms on the twelve test images, which are encoded by a JPEG coder with quality factors (QF) 5 and 80, respectively. Quality factors, which are integers defined in the range 1-100, are indexes of a set of quantization matrices. Larger QF values correspond to better image quality. As can be observed, our proposed dual domain soft decoding technique achieves the best objective performance for all test images and over the low and high quality factors.

More specifically, compared with the image deblocking algorithms, namely, ACR and PSW, the average PSNR gains can be up to 1.95dB and 1.2dB, respectively, which are significant. When comparing with the denoising approaches BM3D-SAPCA, we assume the true quantization error variances are known and fed into this algorithm. As in practice the error variances cannot always be estimated accurately, the results of BM3D-SAPCA shown in Table I-II can be regarded as performance upper bounds. Even under this favorable condition, BM3D-SAPCA is still outperformed by our proposed method, with average PSNR gain being up to 1 dB.

Furthermore, our method works better than the state-of-the-art sparse coding based methods. The average PSNR gain over the KSVD is 0.94dB, with the highest gain being 1.99dB, achieved by the test image *Bike512* when  $QF = 80$ . When comparing with the latest DicTV, our average PSNR gain is 0.99dB when  $QF = 5$ , and the highest gain

1.84dB is retained in the test image *Butterfly* when  $QF = 5$ . For high quality factor  $QF = 80$ , DicTV works poor. Our average PSNR over it is 3.19dB.

We also provide the SSIM [39] performance results of different algorithms in Table I-II. From these tables, we can notice that our method achieves the highest average SSIM scores among all of competing methods. To better demonstrate the superior performance against these compared techniques, we in Fig. 3 illustrate the PSNR comparison for a wide range of QF values from 10 to 90. It can be seen that the proposed method consistently outperforms these competitors for all QF values.

In order to get statistical validation of the superior performance of the proposed method, we further report performance comparison over a large image set. We choose 80 images randomly from UCID dataset,<sup>2</sup> and exam the average PSNR values of compared methods. As illustrated in Fig. 4 and Fig. 5, the proposed method achieves the highest average PSNR values when  $QF = 5$  and  $QF = 80$ , respectively. Furthermore, F-test is conducted in order to demonstrate that our performance is statistically significant. For  $QF = 5$  and  $QF = 80$ , the  $p$ -value is  $5.7129e-12$  and  $8.0875e-35$  respectively, which are both close to zero, indicating that our superior performance is statistically convincing.

### C. Subjective Performance Comparison

In addition to its superior performance in objective fidelity metric, the dual transform-pixel domain restoration approach also obtains better perceptual quality of the restored images. The reader is invited to examine and compare the restored

<sup>1</sup><http://r0k.us/graphics/kodak/>

<sup>2</sup><http://homepages.lboro.ac.uk/~cogs/datasets/ucid/ucid.html>

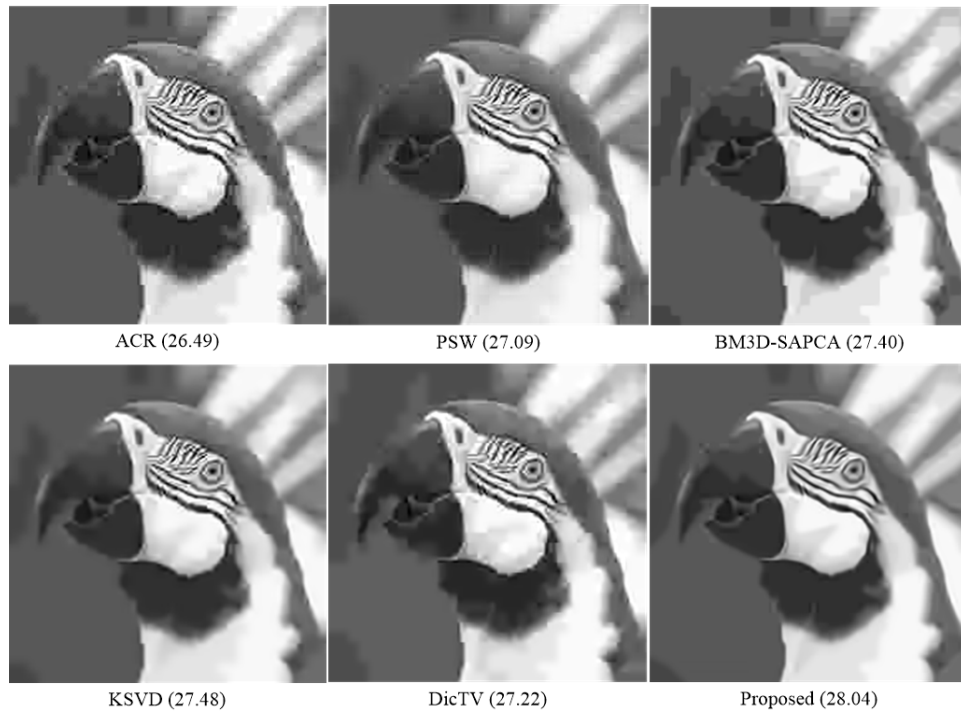


Fig. 7. Comparison of tested methods in visual quality on *Parrot* at  $QF = 5$ . The corresponding PSNR values (in dB) are also shown.

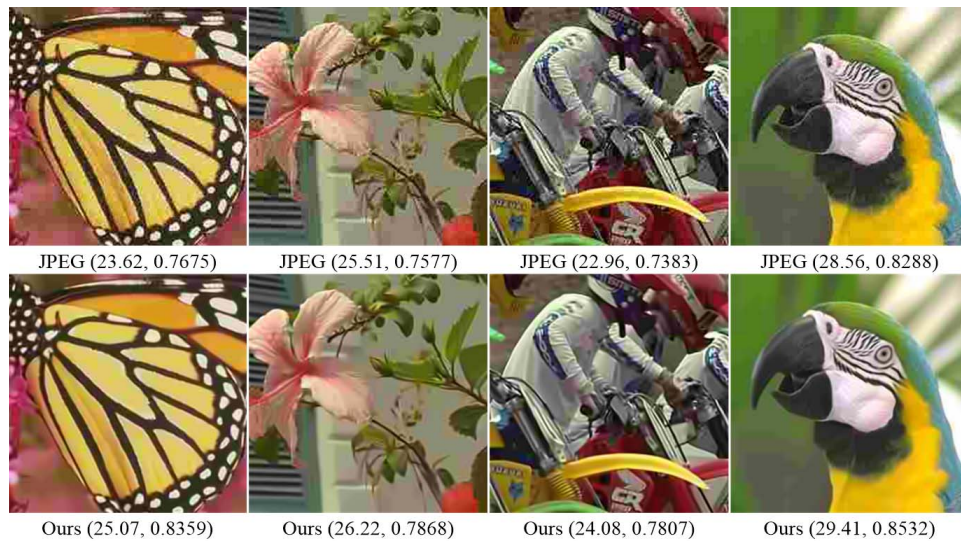


Fig. 8. Restoration of compressed color images, where  $QF = 10$  or  $15$ . The corresponding PSNR (in dB) and SSIM values are also shown.

JPEG images by different methods in Fig. 6-7. It can be seen that the images reconstructed by the ACR algorithm still have strong blocking artifact. In addition, the images reproduced by PSW and BM3D-SAPCA suffer from highly visible noises that accompany edges and textures. KSVD and DicTV can suppress most of blocking artifacts; but there are still noticeable artifacts along edges. This is because patches are processed independently in KSVD and DicTV. When similar patches admit very different estimates, due to the potential instability of sparse decompositions, the quite noticeable reconstruction artifacts appear. In contrast, our new method is capable of restoring images with well-preserved

edges, textures, structures, and sharpness. Even in smooth areas, our approach can still effectively eliminate the blocking artifacts and suppress the staircase and ringing artifacts along edges.

#### D. Restoration of Compressed Color Images

The proposed method can be easily extended to restore compressed color images. When compressing color images, JPEG first performs the YUV color transformation, and then compresses the resulting Y, U and V channels separately. As the image signal energy is highly packed into the luminance channel Y, the proposed dual-domain method

TABLE III  
COMPUTATION COMPLEXITY COMPARISON (IN SECOND) WHEN QF = 5

Image	ACR	PSW	BM3D-SAPCA	KSVd	DicTV	D2SD
<i>Butterfly</i>	1.11	2.82	278.7	335.67	29	101.56
<i>Barbara</i>	0.73	2.81	273.7	138.31	21.59	100.46
<i>Boat</i>	0.71	2.78	269.4	110.46	21.62	97.76
<i>Leaves</i>	0.31	2.29	278.6	553.68	30.28	99.59
<i>Bike</i>	0.57	2.75	286.85	499.98	28.17	103.39
<i>Flower</i>	0.71	2.54	265.12	135.92	22.48	98.65
<i>House</i>	0.89	2.9	268.95	75.85	19.64	106.43
<i>Hat</i>	0.76	2.54	241	73.15	19.79	101.26
<i>Parrot</i>	0.9	2.87	268.1	154.43	21.42	108.29
<i>Average</i>	0.74	2.70	270.04	230.82	23.78	101.93

is applied only to Y. For chrominance channels U and V, we only restore in DCT domain to speed up the process. Fig. 8 shows that the proposed method effectively attenuates the compression artifacts, faithfully preserving the structures in the image.

#### E. Computational Time Comparison

Another issue needed to consider is the computational complexity. Here we show the practical running time comparison on nine  $256 \times 256$  test images when QF = 5. The compared methods are running on a typical laptop computer (Intel Core i7 CPU 2.6GHz, 16G Memory, Win10, Matlab R2014a). As depicted in Table III, the complexity of our method is lower than the state-of-the-art algorithms BM3D-SAPCA and K-SVD.

## VI. CONCLUSION

A novel data-driven sparsity-based approach is proposed for the restoration of compressed images in the dual DCT-pixel domain. The main technical contribution of this work is the combined use of dual dictionaries learned respectively using samples drawn from the hard-decoded input image and samples drawn from uncompressed training images. Experimental results demonstrate the efficacy of the proposed restoration approach for compressed images. The reported research findings reveal so-far under-utilized potential of improving compressed images and videos via sophisticated postprocessing after decompression. In the future work, we will work on simplifying the proposed method to make it more suitable for larger images, e.g., the popular HD images.

## REFERENCES

- [1] X. Liu, X. Wu, J. Zhou, and D. Zhao, "Data-driven sparsity-based restoration of JPEG-compressed images in dual transform-pixel domain," in *Proc. IEEE Conf. CVPR*, Jun. 2015, pp. 5171–5178.
- [2] M. Elad and M. Aharon, "Image denoising via sparse and redundant representations over learned dictionaries," *IEEE Trans. Image Process.*, vol. 15, no. 12, pp. 3736–3745, Dec. 2006.
- [3] J. Yang, J. Wright, T. S. Huang, and Y. Ma, "Image super-resolution via sparse representation," *IEEE Trans. Image Process.*, vol. 19, no. 11, pp. 2861–2873, Nov. 2010.
- [4] W. Dong, L. Zhang, G. Shi, and X. Wu, "Image deblurring and super-resolution by adaptive sparse domain selection and adaptive regularization," *IEEE Trans. Image Process.*, vol. 20, no. 7, pp. 1838–1857, Jul. 2011.
- [5] X. Liu, D. Zhai, D. Zhao, and W. Gao, "Image super-resolution via hierarchical and collaborative sparse representation," in *Proc. IEEE DCC*, Mar. 2013, pp. 93–102.
- [6] X. Wu, D. Gao, G. Shi, and D. Liu, "Color demosaicking with sparse representations," in *Proc. 17th IEEE ICIP*, Sep. 2010, pp. 1645–1648.
- [7] M. Elad, M. A. T. Figueiredo, and Y. Ma, "On the role of sparse and redundant representations in image processing," *Proc. IEEE*, vol. 98, no. 6, pp. 972–982, Jun. 2010.
- [8] J. Mairal, F. Bach, J. Ponce, G. Sapiro, and A. Zisserman, "Non-local sparse models for image restoration," in *Proc. IEEE 12th ICCV*, Sep./Oct. 2009, pp. 2272–2279.
- [9] J. Mairal, M. Elad, and G. Sapiro, "Sparse representation for color image restoration," *IEEE Trans. Image Process.*, vol. 17, no. 1, pp. 53–69, Jan. 2008.
- [10] X. Liu, X. Wu, and D. Zhao, "Sparsity-based soft decoding of compressed images in transform domain," in *Proc. 20th IEEE ICIP*, Sep. 2013, pp. 563–566.
- [11] X. Liu, G. Cheung, X. Wu, and D. Zhao, "Inter-block consistent soft decoding of JPEG images with sparsity and graph-signal smoothness priors," in *Proc. IEEE ICIP*, Sep. 2015, pp. 1628–1632.
- [12] G. M. Farinella and S. Battiato, "On the application of structured sparse model selection to JPEG compressed images," in *Proc. Int. Conf. Comput. Color Imag.*, 2011, pp. 137–151.
- [13] C. Jung, L. Jiao, H. Qi, and T. Sun, "Image deblocking via sparse representation," *Signal Process., Image Commun.*, vol. 27, no. 6, pp. 663–677, 2012.
- [14] H. Chang, M. K. Ng, and T. Zeng, "Reducing artifacts in JPEG decompression via a learned dictionary," *IEEE Trans. Signal Process.*, vol. 62, no. 3, pp. 718–728, Feb. 2014.
- [15] C.-H. Yeh, L.-W. Kang, Y.-W. Chiou, C.-W. Lin, and S.-J. F. Jiang, "Self-learning-based post-processing for image/video deblocking via sparse representation," *J. Vis. Commun. Image Represent.*, vol. 25, no. 5, pp. 891–903, 2014.
- [16] M. Yin, J. Gao, Y. Sun, and S. Cai, "Blocky artifact removal with low-rank matrix recovery," in *Proc. IEEE ICASSP*, May 2014, pp. 1996–2000.
- [17] M. Aharon, M. Elad, and A. Bruckstein, "K-SVD: An algorithm for designing overcomplete dictionaries for sparse representation," *IEEE Trans. Signal Process.*, vol. 54, no. 11, pp. 4311–4322, Nov. 2006.
- [18] K. Dabov, A. Foi, V. Katkovnik, and K. Egiazarian, "Image denoising by sparse 3-D transform-domain collaborative filtering," *IEEE Trans. Image Process.*, vol. 16, no. 8, pp. 2080–2095, Aug. 2007.
- [19] K. Dabov, A. Foi, V. Katkovnik, and K. Egiazarian, "BM3D image denoising with shape-adaptive principal component analysis," in *Proc. Workshop Signal Process. Adapt. Sparse Struct. Represent. (SPARS)*, Saint-Malo, France, Apr. 2009, pp. 1–7.
- [20] P. Chatterjee and P. Milanfar, "Patch-based near-optimal image denoising," *IEEE Trans. Image Process.*, vol. 21, no. 4, pp. 1635–1649, Apr. 2012.
- [21] T. P. O'Rourke and R. L. Stevenson, "Improved image decompression for reduced transform coding artifacts," *IEEE Trans. Circuits Syst. Video Technol.*, vol. 5, no. 6, pp. 490–499, Dec. 1995.
- [22] T. Meier, K. N. Ngan, and G. Crebbin, "Reduction of blocking artifacts in image and video coding," *IEEE Trans. Circuits Syst. Video Technol.*, vol. 9, no. 3, pp. 490–500, Apr. 1999.
- [23] L. Ma, D. Zhao, and W. Gao, "Learning-based image restoration for compressed images," *Signal Process., Image Commun.*, vol. 27, no. 1, pp. 54–65, Jan. 2012.
- [24] X. Zhang, R. Xiong, X. Fan, S. Ma, and W. Gao, "Compression artifact reduction by overlapped-block transform coefficient estimation with block similarity," *IEEE Trans. Image Process.*, vol. 22, no. 12, pp. 4613–4626, Dec. 2013.
- [25] S. S. O. Choy, Y.-H. Chan, and W.-C. Siu, "Reduction of block-transform image coding artifacts by using local statistics of transform coefficients," *IEEE Signal Process. Lett.*, vol. 4, no. 1, pp. 5–7, Jan. 1997.
- [26] H. C. Reeve, III, and J. S. Lim, "Reduction of blocking effect in image coding," in *Proc. IEEE ICASSP*, Apr. 1983, pp. 1212–1215.
- [27] G. Zhai, W. Zhang, X. Yang, W. Lin, and Y. Xu, "Efficient image deblocking based on postfiltering in shifted windows," *IEEE Trans. Circuits Syst. Video Technol.*, vol. 18, no. 1, pp. 122–126, Jan. 2008.

- [28] F. Alter, S. Durand, and J. Froment, "Adapted total variation for artifact free decompression of JPEG images," *J. Math. Imag. Vis.*, vol. 23, no. 2, pp. 199–211, 2005.
- [29] K. Bredies and M. Holler, "A total variation-based JPEG decompression model," *SIAM J. Imag. Sci.*, vol. 5, no. 1, pp. 366–393, 2012.
- [30] Y. Kwon, K. I. Kim, J. Tompkin, J. H. Kim, and C. Theobalt, "Efficient learning of image super-resolution and compression artifact removal with semi-local Gaussian processes," *IEEE Trans. Pattern Anal. Mach. Intell.*, vol. 37, no. 9, pp. 1792–1805, Sep. 2015.
- [31] R. Tibshirani, "Regression shrinkage and selection via the lasso," *J. Roy. Statist. Soc., B (Methodol.)*, vol. 58, no. 1, pp. 267–288, 1996.
- [32] D. I. Shuman, S. K. Narang, P. Frossard, A. Ortega, and P. Vandergheynst, "The emerging field of signal processing on graphs: Extending high-dimensional data analysis to networks and other irregular domains," *IEEE Signal Process. Mag.*, vol. 30, no. 3, pp. 83–98, May 2013.
- [33] X. Liu, D. Zhai, D. Zhao, G. Zhai, and W. Gao, "Progressive image denoising through hybrid graph Laplacian regularization: A unified framework," *IEEE Trans. Image Process.*, vol. 23, no. 4, pp. 1491–1503, Apr. 2014.
- [34] S. Gao, I. W.-H. Tsang, and L.-T. Chia, "Laplacian sparse coding, hypergraph Laplacian sparse coding, and applications," *IEEE Trans. Pattern Anal. Mach. Intell.*, vol. 35, no. 1, pp. 92–104, Jan. 2013.
- [35] M. Zheng *et al.*, "Graph regularized sparse coding for image representation," *IEEE Trans. Image Process.*, vol. 20, no. 5, pp. 1327–1336, May 2011.
- [36] H. Lee, A. Battle, R. Raina, and A. Y. Ng, "Efficient sparse coding algorithms," in *Proc. NIPS*, 2007, pp. 801–808.
- [37] G. Zhai, W. Zhang, X. Yang, W. Lin, and Y. Xu, "Efficient deblocking with coefficient regularization, shape-adaptive filtering, and quantization constraint," *IEEE Trans. Multimedia*, vol. 10, no. 5, pp. 735–745, Aug. 2008.
- [38] H. Zou and T. Hastie, "Regularization and variable selection via the elastic net," *J. Roy. Statist. Soc., B (Statist. Methodol.)*, vol. 67, no. 2, pp. 301–320, 2005.
- [39] Z. Wang, A. C. Bovik, H. R. Sheikh, and E. P. Simoncelli, "Image quality assessment: From error visibility to structural similarity," *IEEE Trans. Image Process.*, vol. 13, no. 4, pp. 600–612, Apr. 2004.



**Xianming Liu** (M'12) received the B.S., M.S., and Ph.D. degrees in computer science from the Harbin Institute of Technology (HIT), Harbin, China, in 2006, 2008, and 2012, respectively. In 2007, he joined the Joint Research and Development Laboratory, Chinese Academy of Sciences, Beijing, as a Research Assistant. From 2009 to 2012, he was with the National Engineering Laboratory for Video Technology, Peking University, Beijing, as a Research Assistant. In 2011, he spent half a year with the Department of Electrical and Computer

Engineering, McMaster University, Canada, as a Visiting Student, where he was a Post-Doctoral Fellow from 2012 to 2013. He has been a Project Researcher with the National Institute of Informatics, Tokyo, Japan since 2014. He is an Associate Professor with the Department of Computer Science, HIT. He has published over 40 international conference and journal publications, including top IEEE journals, such as the IEEE TRANSACTIONS ON IMAGE PROCESSING, the IEEE TRANSACTIONS ON CIRCUITS AND SYSTEMS FOR VIDEO TECHNOLOGY, the IEEE TRANSACTIONS ON INFORMATION FORENSICS AND SECURITY, and the IEEE TRANSACTIONS ON MULTIMEDIA; and top conferences, such as CVPR, IJCAI, and DCC.



**Xiaolin Wu** (M'88–SM'96–F'11) received the B.Sc. degree in computer science from Wuhan University, China, in 1982, and the Ph.D. degree in computer science from the University of Calgary, Canada, in 1988. He started his academic career in 1988, and has been a Faculty Member with the University of Western Ontario, New York Polytechnic University. He is currently with the Department of Electrical and Computer Engineering, McMaster University, Hamilton, ON, Canada, as a Professor, and holds the NSERC-DALSA Industrial Research Chair in Digital Cinema. He has authored over 180 research papers and holds two patents in these fields. His research interests include image processing, multimedia compression, joint source-channel coding, multiple description coding, and network-aware visual communication.



**Jiantao Zhou** (M'11) received the B.Eng. degree from the Department of Electronic Engineering, Dalian University of Technology, Dalian, China, in 2002, the M. Phil. degree from the Department of Radio Engineering, Southeast University, Nanjing, China, in 2005, and the Ph.D. degree from the Department of Electronic and Computer Engineering, Hong Kong University of Science and Technology, Hong Kong, in 2009. He held various research positions with the University of Illinois at Urbana-Champaign, the Hong Kong University of Science and Technology, and McMaster University. He is currently an Assistant Professor with the Department of Computer and Information Science, Faculty of Science and Technology, University of Macau. He holds three granted U.S. patents and two granted Chinese patents. His research interests include multimedia security and forensics, and high-fidelity image compression. He was a co-author of a paper that received the best paper award in the IEEE Pacific-Rim Conference on Multimedia in 2007.



**Debin Zhao** received the B.S., M.S., and Ph.D. degrees in computer science from the Harbin Institute of Technology, China, in 1985, 1988, and 1998, respectively. He is currently a Professor with the Department of Computer Science, Harbin Institute of Technology. He has authored over 200 technical articles in refereed journals and conference proceedings in the areas of image and video coding, video processing, video streaming and transmission, and pattern recognition.